

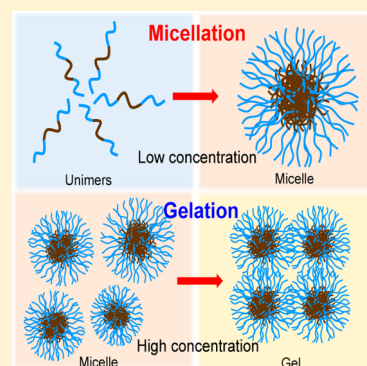
Role of Solvent Water in the Temperature-Induced Self-Assembly of a Triblock Copolymer

Achintya Kundu,¹ Pramod Kumar Verma,¹ and Minhaeng Cho*^{1,2}

Center for Molecular Spectroscopy and Dynamics, Institute for Basic Science (IBS), Seoul 02841, Republic of Korea
Department of Chemistry, Korea University, Seoul 02841, Republic of Korea

Supporting Information

ABSTRACT: Water-soluble triblock copolymers have received much attention in industrial applications and scientific fields. We here show that femtosecond mid-IR pump–probe spectroscopy is useful to study the role of water in the temperature-induced self-assembly of triblock copolymers. Our experimental results suggest two distinct subpopulations of water molecules: those that interact with other water molecules and those involved in the hydration of a triblock copolymer surface. We find that the vibrational dynamics of bulk-like water is not affected by either micellation or gelation of triblock copolymers. The increased population of water interacting with ether oxygen atoms of the copolymer during the unimer to micelle phase transition is important evidence for the entropic role of water in temperature-induced micelle formation at a low copolymer concentration. In contrast, at the critical gelation temperature and beyond, the population of surface-associated water molecules interacting with ether oxygen atoms decreases, which indicates important enthalpic control by water. The present study on the roles of water in the two different phase transitions of triblock copolymers sheds new light on the underlying mechanisms of temperature-induced self-aggregation behaviors of amphiphiles that are ubiquitous in nature.



Block copolymers are polymers composed of repeating units of two or more different monomers. Block copolymers having both hydrophilic and hydrophobic repeat units show a rich diversity in phases and self-assembly structures. Therefore, they have been used for many industrial applications in detergent, dispersion stabilization, foaming, emulsification, lubrication, and so on.^{1,2} Their important uses are also found in pharmaceuticals for drug solubilization and controlled release, in bioprocessing application for protecting microorganisms against mechanical damage, in analytical chemistry of separating organic compounds from aqueous solutions, and in developing microreactors for reactions that are not favored in either aqueous solutions or organic solvents.^{1–3} Because water is the solvent for most of the triblock copolymer solutions and water plays a major role in many self-assembly processes, it becomes essential to understand how the water hydrogen-bonding (H-bonding) network structure and dynamics are modulated in different structural phases of block copolymers.

One of the most commonly used and studied triblock copolymers is Pluronic, which is known as P123 (poly(ethylene oxide)₂₀–poly(propylene oxide)₇₀–poly(ethylene oxide)₂₀). It consists of hydrophilic PEO (poly(ethylene oxide)) and comparatively hydrophobic PPO (poly(propylene oxide) blocks (see Figure 1a for the molecular structure of amphiphilic P123). Because of the hydrophilic–hydrophobic–hydrophilic structure of the P123 chain, it exhibits very interesting and unique self-aggregation behavior when dissolved in water. In fact, it has been investigated by using a variety of experimental methods, such as small-angle neutron scattering,

static light scattering, time-resolved fluorescence spectroscopy, and so on.^{4–7} The polymer remains mostly as unimers at low concentrations and below the critical micelle temperature (CMT = 290 K for P123).⁶ As the temperature increases beyond the CMT, unimers start to form micelles spontaneously.^{6,7} Furthermore, upon increasing concentration, the micellar solution becomes gel-like and remains in the gel phase over a wide range of temperatures from 290 to 320 K.⁸

As per a small-angle neutron scattering study, the average size of spherical micelles is about 8 nm and the hydrophobic core of the micelle mainly consists of PPO blocks, whereas the hydrophilic corona region is occupied by PEO blocks (Figure 1b). In the gel phase at high concentrations, the distance between centers of neighboring micelles is about 14 nm, which is smaller than twice (16 nm) the radius of a single micelle. This suggests that the corona regions of neighboring micelles are spatially overlapped and partly entangled with each other (Figure 1c).^{5,7,9} It is this phase diversity of the P123–water system that is the main interest in the present work. To elucidate the role of solvent water in temperature-induced self-assembly processes, we carried out time-resolved IR pump–probe (PP) measurements and show the direct interplay between the water H-bonding structural change and the phase transitions of P123 in aqueous solutions.

Received: April 25, 2017

Accepted: June 14, 2017

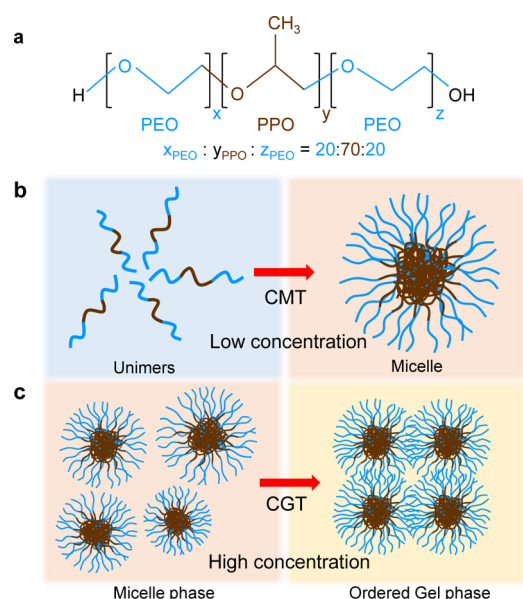


Figure 1. (a) Molecular structure of a triblock copolymer composed of PEO and PPO and denoted as $(PEO)_x-(PPO)_y-(PEO)_z$. (b) Schematic representation of the unimer to micelle phase transition at the critical micelle temperature (CMT). (c) Schematic representation of the micelle to ordered gel phase transition at the critical gelation temperature (CGT).

Previous attempts to understand the microenvironment of the self-assembled P123^{5,10–12} used fluorescence anisotropy measurement method because the anisotropy decay in time provides critical information on the local environment around each fluorophore. For instance, Dutt et al. measured temperature-dependent rotational diffusion constants of hydrophobic fluorescent molecules, 2,5-dimethyl-1,4-dioxo-3,6-diphenylpyrrolo[3,4-*c*]pyrrole and 1,4-dioxo-3,6-diphenylpyrrolo[3,4-*c*]pyrrole, in 1% (w/v) P123 solution. Although the fluorescence anisotropy signal at temperature lower than CMT decays single-exponentially, its decay at higher temperature above the CMT becomes bi-exponential. This was suggested to be critical evidence for the coexistence of two different microenvironments around the P123 micelle.⁴ As the concentration of P123 further increases up to 30% (w/v) in water, the micellar system behaves like a gel, and time-resolved (both femtosecond and picosecond) fluorescence studies of coumarin with varying excitation wavelengths were performed to extract the solvation dynamics at different microenvironments in the gel-phase solution. It was found that the solvation dynamics is slower at the surface of the P123 compared to that in bulk water,⁵ indicating that the water network structure at the surface of gel phase P123 micelles is quite different from that in bulk water. Although various fluorophores have been of great use in studying local environments, the fluorophore is not a direct probe of a water H-bonding network and naturally it forms specific interactions with chemical groups of the block copolymers. Consequently, the results from time- and frequency-resolved fluorescence measurements are prone to depend on a specific fluorescence dye molecule.

Here, we address the question about how the water H-bonding structure and the extent of hydration of block copolymer subunits change with temperature and P123 concentration in aqueous solutions by using femtosecond IR PP technique, which enables direct measurements of vibrational

and rotational dynamics of water molecules.^{13–23} The OD stretch mode of HDO has long been considered an excellent IR probe for water and has been widely used in studying ultrafast water H-bonding making and breaking dynamics in a number of aqueous solutions containing micelles, amphiphilic mixtures,^{24,25} reverse micelles,^{26–31} polymers,^{18,23} lipid multibilayers,^{13,20,21,32,33} lamella, and so forth.^{19,34} In this Letter, we present the polarization-controlled IR PP results for aqueous P123 solutions at two different concentrations (1 and 23 wt %) with varying temperature to study the phase transitions from unimers to micelles and from micelles to the gel phase (see Figure 1b,c).

The background-subtracted FTIR spectra of the OD stretch mode of HDO in 1 and 23 wt % P123 solutions at different temperatures are shown panels (a) and (c) of Figure 2,

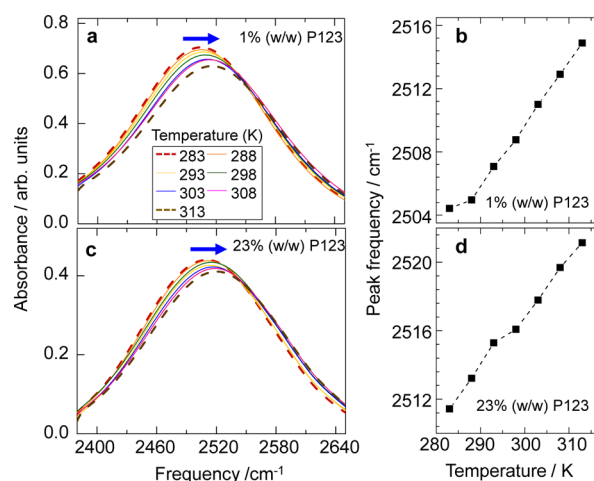


Figure 2. Background-subtracted FTIR spectra of the OD stretch mode of HDO in 1 (a) and 23 wt % (c) P123 solutions. The peak frequency of each FTIR spectrum is plotted with respect to temperature (b,d). Dashed lines in (b) and (d) are to guide the eye.

respectively. As the P123 concentration increases from 1 to 23 wt %, the peak position of the OD stretch IR band undergoes a blue shift by about 8 cm⁻¹ (see Figure S1 in the Supporting Information (SI)). Note that the number of water molecules per ether oxygen atom of P123 is approximately 284 and 10 in the cases of the 1 and 23 wt % P123 solutions, respectively. Thus, the increased absorbance on the blue side of the OD stretch IR spectrum signifies a change and breaking of the tetrahedral water H-bonding network due to an increased OD–ether population. The reduced electric field along the OD bond of HDO bound to the ether oxygen atom increases the OD stretch frequency (blue shift) much like the case of HDO molecules interacting with ions in salt solutions.^{35–37} A similar concentration-dependent blue shift of the OD stretch IR band with increasing macromolecule crowder (poly(ethylene glycol)-dimethyl ether) concentration has also been observed and reported by us recently.¹⁸

For both 1 and 23 wt % P123 solutions, the OD stretch band is blue-shifted upon increasing the temperature from 283 to 313 K by about 10 cm⁻¹ regardless of the P123 concentration. For the sake of direct comparison, we have also measured the temperature-dependent spectra of the OD stretch mode in neat water (Figure S2) and found that the magnitude of the blue shift is about 10 cm⁻¹, which is in agreement with the earlier temperature-dependent study for the OD stretch mode of

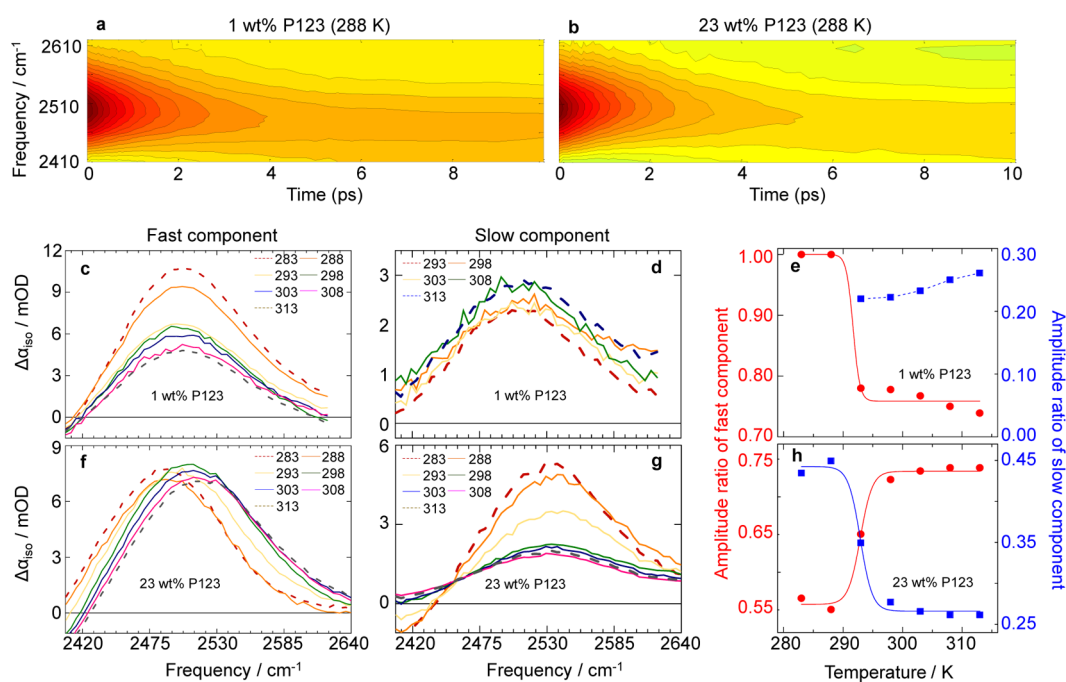


Figure 3. Isotropic IR PP signal of the OD stretch mode of HDO in 1 (a) and 23 (b) wt % P123 solutions at 288 K. Decomposed isotropic IR PP eigenspectra are shown in (c), (d), (f), and (g). Below 290 K, in the case of the 1 wt % P123 solution, the isotropic IR PP signal decays single exponentially. Above 290 K, the isotropic IR PP time profiles should be fitted with bi-exponentially decaying functions. Amplitude ratios are plotted with respect to temperature in (e) and (h) for the 1 and 23 wt % P123 solutions, respectively. The sigmoidal lines in (e) and (h) are shown to guide the eye.

HDO.³⁸ The blue shift of the OD stretch IR band with respect to increasing temperature results from the decrease of both the H-bond number and strength due to the increased thermal fluctuation. In addition, the experimentally observed decrease in the absolute absorbance of the OD stretch mode with increasing temperature can also be explained by considering a non-Condon effect, that is, coordinate dependence of the transition moment. Note that the low-frequency OD stretch mode has a larger oscillator strength due to the polarizable nature of the water molecule.^{38,39}

Now, we focus on the vibrational relaxation process of the OD stretch mode. Previously, we investigated the intra- and intermolecular energy transfer pathways by carrying out quantum mechanical/molecular mechanical MD simulations and applying the kinetic energy spectral density calculation method to the MD trajectory analyses. There, we found that the vibrationally excited OD stretch mode of HDO in water initially transfers its excess energy to the HDO bending mode followed by relaxations to other intramolecular modes and to neighboring H-bonded water molecules.⁴⁰ In general, it is well-known that the vibrational relaxation of the OD stretch mode of HDO depends on the local electrostatic environment.⁴¹ Here, the isotropic IR PP data provide information on the rate of vibrational population relaxation. In aqueous P123 solutions, HDO can interact with other water hydroxyl groups (OD-w) or with ether oxygen atoms of P123 (OD-e). Clearly, the OD group of HDO H-bonded to another water molecule differs from that H-bonded to ether oxygen of P123 by the set of coupled intramolecular modes and the effective bath density of states absorbing the OD vibrational energy. Consequently, the associated vibrational relaxation mechanisms and rates of OD-w and OD-e may well be different from each other. To prove this, we first obtained the isotropic IR PP spectra of HDO in isotopically diluted solutions and plotted them in Figure 3a for

the 1 wt % P123 solution and in Figure 3b for the 23 wt % P123 solution, both at 288 K, where the red color represent the ground-state bleach (GSB) and stimulated emission (SE). In Figures S3 and S4 in the SI, the IR PP spectra taken at several PP delay times are shown with fitting results and the eigenspectra of the decaying components and one ingrowing thermal heating component. The heating contribution resulting from an increase of local temperature around HDO due to the vibrational energy relaxation (VER) of the pump-excited OD stretch mode contributes to the IR PP data at long delay times. This can be easily removed by fitting the isotropic PP data with the kinetic relaxation model proposed by Bakker and co-workers.^{14,42}

The isotropic PP data for the OD stretch mode of HDO in neat water is nicely fitted with a single-exponentially decaying function with a decay time constant of 1.6 ps, which is the OD stretch vibrational lifetime of HDO in neat water. In the case of the 1 wt % P123 solution, the isotropic PP data at 283 and 288 K can be described by a single-exponential decay. However, at temperatures higher than 290 K (>CMT), two decay components should be considered to fit the data (Figure S3e in the SI). Note that even at temperatures lower than the CMT, one cannot completely rule out the possibility of dimer or small cluster formation. However, because the micellation of P123 is a *critical* aggregation process exhibiting a sudden change in the population distribution of aggregates at its critical temperature, the relative populations of small size clusters would be negligibly smaller than that of unimers at temperatures below the CMT. Therefore, it is believed that the presence of dimers and small clusters would not significantly affect the fitting analysis results.

The decomposed isotropic PP spectra of the fast and slow components at different temperatures are shown in Figure 3c,d for the 1 wt % P123 solution. Previously, we reported the IR PP

spectra of the OD stretch mode of HDO in salt solutions at various salt concentrations and estimated the relative populations of two different types of OD stretch modes that are OD–water and OD–anion forms. It is well-known that the transition dipole moment of the OD stretch mode depends on the frequency or local electrostatic environment. Thus, its IR spectrum differs from the Raman scattering spectrum, which is known as IR–Raman noncoincidence.^{43,44} The frequency dependence of the OD stretch IR intensity was taken into account in estimating the populations of OD–water and OD–anion species, but we found no notable difference from the estimated populations obtained without considering it. This is not because the frequency dependence of the OD stretch IR intensity is weak but because the integrated areas obtained after carrying out global fitting analyses are not very sensitive to the frequency dependence of the OD transition dipole moment. Therefore, here, for the sake of simplicity, we assume that the OD transition dipole moment does not strongly depend on frequency, and the relative fractions of the two components extracted from the integrated areas of the respective PP eigenspectra are plotted with respect to temperature in Figure 3e. In addition, the vibrational lifetimes of the fast and slow components in the 1 wt % P123 solution are plotted with respect to temperature in Figure 4a. The vibrational lifetime of

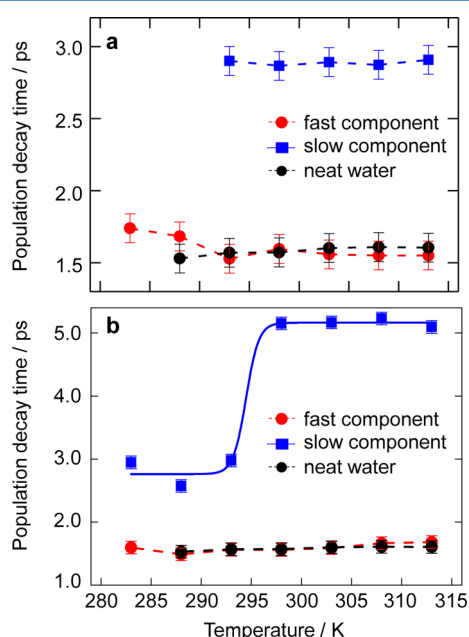


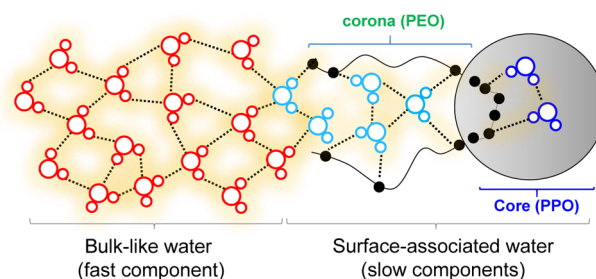
Figure 4. Vibrational lifetimes of the OD stretch mode of HDO with respect to temperature in 1 (a) and 23 wt % (b) P123 solutions. For comparison, we also plot the temperature-dependent vibrational lifetime of the OD stretch mode of HDO in neat water (black circles). The sigmoidal fit curve in (b) is to guide the eye.

the fast component appears to be independent of temperature, and its value (1.6 ps) is quite similar to the OD stretch lifetime of HDO in neat water.^{45,46} For the sake of direct comparison, we have additionally measured the isotropic IR PP data of HDO in neat water at various temperatures and plotted the OD stretch vibrational lifetime with respect to temperature in Figures 4a,b (black circles). Note that the vibrational lifetime of the OD stretch mode of HDO in neat water does not depend on temperature, which corroborates with the results obtained by Tokmakoff and co-workers,³⁸ where they observed only a

marginal increase (approximately 0.3 ps) in the vibrational lifetime of the OD stretch mode of HDO as the temperature increased from 278 to 320 K. Therefore, from Figure 4a, it is clear that the fast decay component relaxing on a time scale similar to that of HDO in neat water can be assigned to the VER of OD–w in the bulk-like water phase. The IR PP eigenspectra of the fast component shifts to higher wavenumbers (blue shift) with increasing temperature, which is again consistent with the experimental observation that the IR PP spectrum of HDO in neat water undergoes a blue shift with increasing temperature (see Figure S5 in the SI).

An important observation here is that the slow component with a decay time constant of ~ 2.9 ps appears only at a temperature higher than CMT, when the copolymer concentration is 1 wt %. The slowly relaxing component can be assigned to the VER of OD–e water molecules inside of the corona region of each micelle spontaneously formed through the self-aggregation of P123 unimers (Scheme 1). The relative

Scheme 1. Schematic Representation of Different Water Phases^a



^aBulk-like water and surface water.

population of this slow component, estimated from the integrated IR PP spectra, is found to be less than 30% at any temperature (blue squares in Figure 3e). Furthermore, the peak position of the IR PP eigenspectrum of the slow component is negligibly dependent on temperature. These two observations are strong evidence that the slow component cannot be assigned to water molecules forming tetrahedral H-bonding interactions with other bulk-like water molecules (Scheme 1).

Although at temperatures below 290 K each P123 unimer has water molecules interacting with ether oxygen atoms, they behave like bulk water as their vibrational lifetime is close to that in neat water. This indicates that water molecules hydrating each P123 unimer are surrounded by water molecules forming a bulk-like water H-bonding network. This is not unexpected because at 1 wt % P123 concentration ~ 284 water molecules are available per ether. However, at 293 K and onward, the unimers aggregate and form micelles even at this low P123 concentration. Interestingly, such unimer to micelle transition induced by increasing temperature is clearly observed in our IR PP signal with the appearance of a new (slow) component, even though the ratio of water molecules to ether oxygen atoms of P123 is still 284:1. Previously, such double-exponential decay of the IR PP signal has also been found in similar systems such as reverse micelles formed by Igepal CO-520, where the polar head parts of the Igepal reverse micelle structurally resemble the outer corona region of the P123 micelle because they both have ethylene oxide segments.^{47,48} In the case of the Igepal reverse micelle, the fast component (1.8 ps) was assigned to bulk-like water molecules, whereas the slow

component with a decay time constant of 3.2 ps is from water molecules interacting with the polar head groups of the Igepal reverse micelle.^{47,48} Similarly, the two components in our P123 solution with micelles can be assigned to water molecules in a bulk-like water environment and those interacting with ether oxygen atoms of the P123 in the corona and core regions of micelle.

The temperature-induced unimer to micelle transition (or the transition from a state with disordered, randomly distributed P123 unimers to a state with ordered self-assembled micelles) at low P123 concentration (1 wt%) accompanies or is driven by an increased population of water molecules with fewer H-bonded water molecules inside of the corona or at the surface of the P123 micelle. Because the H-bonding interaction energy between two water molecules is larger than that between a water molecule and an ether oxygen atom of P123, the transition from unimers to micelles is enthalpically disfavored. Consequently, our experimental observation indicates that this temperature-induced self-assembly to form P123 micelles through the aggregation of unimers is mostly an entropy control effect.

At a high P123 concentration (23 wt %), the isotropic IR PP signals at all temperatures should be described with two decaying components. The fitted isotropic IR PP spectra of HDO in the 23 wt % P123 solution at 283 K are shown in Figure S4a, and the eigenspectra and the kinetic traces of the two decay components with one ingrowing heating component are shown in Figure S4b,c, respectively. The eigenspectra of the fast and slow components at different temperatures are shown in Figure 3f,g. In Figure 4b, the vibrational lifetimes of these two decay components are plotted with respect to temperature.

The fact that the peak frequency of the fast component (Figure 3f) undergoes a blue shift with increasing temperature and the time constant of the fast component is quantitatively similar to that of HDO in neat water led us to conclude that the fast component, of which the decay constant does not strongly depend on temperature, originates from water molecules in a bulk water-like environment even when the highly concentrated P123 polymers form either micelles (at low temperature below 295 K) or ordered gel phase aggregates (at high temperature above 295 K). What is surprising to us is the temperature-dependent decay time constant of the slow component. It is about 2.9 ps at lower temperatures than 295 K, where P123 polymers are predominantly in the micellar phase. This slow component can be assigned to water molecules residing mostly near ether oxygen atoms in the corona region of the micelle with a relatively small population of water molecules in the core region formed by PPO blocks (as shown in Scheme 1). As the temperature increases beyond 295 K (critical gelation temperature, CGT), the decay time constant increases to 5.2 ps, which indicates that the water molecules in the corona and core regions of micelles forming large-scale and relatively ordered aggregates in the gel phase have very different local electrostatic environments as compared to those interacting with ether oxygen atoms of P123 in micelle-phase solutions at low temperatures (<295 K). This notable temperature dependence of the decay time constant of the slow component is correlated with the phase transition from the micelle- to gel phase solutions, which is also manifested by the relative population of the fast and slow components extracted from the two-component analyses of the IR PP data (see Figure 3h). Note that the population of bulk-like water increases with a significant population decrease of OD-e water molecules

present in loosely packed P123 micelles in micellar solution (P123 concentration: 23 wt %; $T < 295$ K).

In micelle solutions (at $T < 295$ K and a concentration of 23 wt %), spherical micelles with an average radius of 8 nm are loosely packed. Now, upon further increasing the temperature to higher than 295 K, micelles approach close to one another and the average distance between two neighboring micelles is reduced to 14 nm, which is 2 nm smaller than twice the radius of each individual micelle. Such a tight packing structure of micelles in the gel phase causes the PEO segments of P123 polymers in its corona region to overlap with those in neighboring micelles, which therefore expels some of the water molecules out of the corona regions in ordered micelle aggregates. This redistribution of water molecules induced by gel phase formation in highly concentrated triblock copolymer solutions is clearly observed in our estimated (relative) fractions of the fast (bulk-like water molecules) and slow (surface-associated and isolated water molecules) components (see Figure 3h). Indeed, the relative fractions of the two components undergo sharp transitions at around 295 K, indicating that water H-bonding structure and the VER mechanism abruptly change and directly reflect the phase transition of the 23 wt % P123 solution from the spatially dispersed micelle phase to the ordered self-aggregation (gel) phase.

In addition to the isotropic IR PP data, the anisotropy decay data are of essential use in identifying very slow (in rotational motion) water molecules in the corona and/or core regions of P123 micelles because the water rotational dynamics strongly depends on the local H-bonding environment. The reorientational motion of a single water molecule involves concerted breaking and re-forming of H-bonds of those water molecules in a bifurcated H-bond configuration with two other nearby water molecules (incoming and outgoing).^{49,50} The anisotropy decays of the OD stretch mode of HDO in two different solutions at 1 and 23 wt % P123 concentrations are shown in Figure S6, where the parallel and perpendicular IR PP signals at the positive peak frequencies were used to calculate the time-dependent anisotropy values. In the 1 wt % P123 solution, the anisotropy decay is always well fitted with a single-exponential function. This monoexponential decay of the anisotropy signal for 1 wt % P123 solution is consistent with the fact that a significant fraction (almost 70%) of water molecules relaxes on a time scale similar to that in neat water. Furthermore, the rotational time scale of OD-e water molecules in the corona region of micelles at low P123 concentrations is not time scale-separable from that of OD-w in a bulk-like water environment. Nonetheless, the rotational time constant does depend on temperature (Figure 5a). For direct comparison, we measured the reorientational relaxation of HDO in neat water in the temperature range from 288 to 313 K. The water reorientational time (Figure S7 in the SI) decreases from 2.1 ± 0.1 (at 288 K) to 1.5 ± 0.1 ps (at 313 K) in neat water. This temperature dependence of the water reorientational time with respect to temperature in neat water is almost the same as that in the 1 wt % P123 solution.

However, in the 23 wt % P123 solution, the anisotropic decay signal cannot be described with a single-exponential function due to the presence of a very slow (almost constant in time) component (>10 ps), which can better be modeled as an offset, that is, $r(t) = R_0 \exp(-t/\tau_{\text{rot}}) + R_{\text{slow}}$. Here, τ_{rot} is the rotational relaxation time constant due to OD-w in a bulk-like water environment, whereas the slow component whose

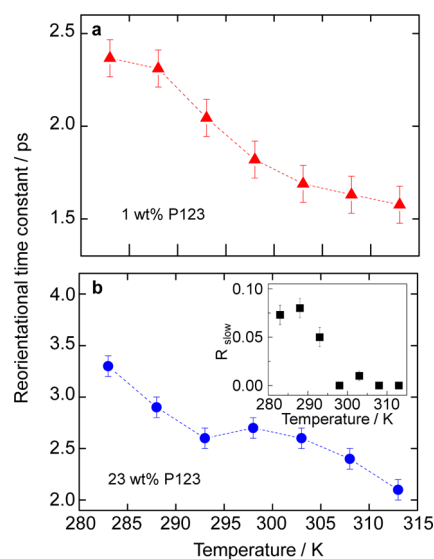


Figure 5. Reorientational time constant of the OD stretch mode of HDO in 1 (a) and 23 wt % (b) P123 solution at different temperatures. The inset in (b) shows the R_{slow} values at different temperatures. Dashed lines are to guide the eye.

amplitude is R_{slow} corresponds to the relative population of water molecules bound to ether oxygen atoms of P123 in micelles. Note that the slow offsets in the anisotropy signals are observed only in the temperature below 295 K (see the inset in Figure 5b). As the temperature increases above 295 K, micelles are entangled and form large-scale gel phase aggregates. Then, the water molecules initially on the surface of micelles are forced to move out toward the bulk-like water phase (Figure 3f). Consequently, a significant fraction (almost 75%) of water molecules vibrationally relaxes on a time scale similar to that in neat water, which is, we believe, the reason why we could not see the corresponding slow component at temperatures higher than 295 K. The τ_{rot} values were found to be 2.3 and 3.4 ps for the 1 and 23 wt % P123 solutions, respectively, at 283 K. A marginal slowdown of the anisotropy decay when the P123 concentration is increased clearly indicates that the H-bonding structure in bulk-like water is little perturbed even in the 23 wt % P123 solution. In fact, the increase of the anisotropy decay constant when the concentration increases from 1 to 23 wt % could be just related to an increase in the viscosity of the solution. The temperature dependence of τ_{rot} in the 23 wt % P123 solution is again similar to that in neat water.

Here, we have shown that the IR PP measurement method is of exceptional use for tracing the phase transitions of self-assembled block copolymers in aqueous solutions by monitoring changes in vibrational dynamics of solvent water. Interestingly, the fraction of bulk-like water molecules increases upon increasing the temperature beyond the CGT, with a simultaneous increase of population in highly compact micellar aggregates. Therefore, in stark contrast to the micellar transition from unimers to micelles at low P123 concentrations, which is mainly driven by the entropic control of water, the gelation transition from the micelle to gel phase at high P123 concentrations is determined by enthalpic control. Note that the water molecules with high entropy in dispersed loosely packed micelles disappears, and both bulk-like water and tightly bound water inside of micelle aggregates in the gel phase become more populated at an elevated temperature higher than the CGT. Therefore, we here show that a single mechanism

does not apply to the explanations of both temperature-induced self-assembling phenomena exhibited by block copolymers.

Thermodynamically, an elevated temperature of any composite system causes a shift of balance toward a higher entropy state.⁵¹ For instance, as the temperature increases beyond the melting point, globular proteins undergo a conformational transition from an ordered and nicely packed tertiary or even quaternary structure with low entropy to a highly disordered unfolded state with significantly higher entropy.^{52,53} However, the temperature-induced self-assembly observed in the P123 solutions is the opposite because, upon increasing the temperature, an ordered assembled structure, for example, a micelle, with low entropy is favored over the disordered randomly distributed unimers state. This seemingly counterintuitive phenomenon was explained by considering entropic control by water.^{7,54} Below the critical aggregation temperature (CAT), water molecules around hydrophobic particles, molecules, or polymers have ordered structures with small entropy. Upon increasing the temperature beyond the CAT, they form aggregates with net reduced surface areas, which restores the water H-bonds, and the water molecules with high entropy increases. Therefore, the net increase of water entropy during the self-aggregation process exceeds the entropy decrease of self-assembling hydrophobic particles or molecules. This entropy control mechanism involving a dramatic change of water entropy upon temperature-induced self-assembly has long been accepted as the most successful description.

However, none of the previous experiments provided clear and quantitative evidence for the coexistence of two or more different types (or phases) of water molecules having quite different environments. In the present work, we could identify at least three different water phases that are (i) bulk-like water with an OD vibrational lifetime of 1.6 ps, (ii) loose micellar water with an OD vibrational lifetime of 2.9 ps, and (iii) water in tightly packed micelle aggregates in a gel phase with an OD vibrational lifetime of 5.2 ps. On the basis of our experimental results and subsequent interpretations presented above, we found that the temperature-induced phase transition from unimers to micelles at low P123 concentrations is due to the entropic effect of water, where the water entropy increase is larger than the entropy decrease due to the formation of ordered micelles. On the other hand, the temperature-induced phase transition from micelles to ordered micelle aggregates in the gel phase cannot be described by solely considering the water entropic control mechanism because the enthalpic effect originating from newly formed (restored) water–water H-bonds in the bulk-like water phase becomes important and dominant.

Although the P123 micellar solution at low copolymer concentration and the P123 gel phase solution at high copolymer concentration are homogeneous and isotropic, we here show that more than one water phase can exist with different vibrational properties reflecting different local environments and water H-bonding structures. The changes in the water H-bonding structure and dynamics revealed by our IR PP data are found to be in direct correlation with the phase transitions of the triblock copolymer. The emergence of slowly relaxing IR PP components in micelle and gel phases of aqueous P123 solutions shows that there exists a large amount of water molecules in the corona or surface regions of micelles and ordered gel phase solutions. Those confined water molecules could play an important role in chemical reactions

occurring inside of the P123 microreactors. Furthermore, the present work provides direct evidence for two different roles of solvent water in temperature-induced self-assembly processes in aqueous P123 solutions at low and high concentrations. It becomes clear that a delicate balance between entropic and enthalpic controls by water is the key to understanding self-assembly induced by temperature. Currently, we are carrying out a new set of experiments with a different IR probe, for example, HN_3 , to gain more insight into the interplay between the self-assembly structure of P123 and the local electrostatic environments. We strongly anticipate that the present study on the water H-bond network structure and dynamics in such a reversible phase transition system can shed light on the role and effects of water on the more general and ubiquitous self-assembling phenomena in nature.

■ ASSOCIATED CONTENT

Supporting Information

The Supporting Information is available free of charge on the ACS Publications website at DOI: [10.1021/acs.jpcllett.7b01008](https://doi.org/10.1021/acs.jpcllett.7b01008).

FTIR spectra of the OD stretch mode of HDO in neat water as well as 1 and 23 wt % P123 solutions at 283 K, IR PP data and decomposed eigenspectra, IR PP time profiles and fitting results, and anisotropic IR PP data and rotational time constants with respect to temperature (PDF)

■ AUTHOR INFORMATION

Corresponding Author

*E-mail: mcho@korea.ac.kr.

ORCID

Achintya Kundu: [0000-0002-6252-1763](https://orcid.org/0000-0002-6252-1763)

Pramod Kumar Verma: [0000-0001-8837-3167](https://orcid.org/0000-0001-8837-3167)

Minhaeng Cho: [0000-0003-1618-1056](https://orcid.org/0000-0003-1618-1056)

Notes

The authors declare no competing financial interest.

■ ACKNOWLEDGMENTS

This work was supported by IBS-R023-D1. All mid-IR PP measurements were performed in the Seoul center of Korea Basic Science Institute (KBSI).

■ REFERENCES

- (1) Schmolka, I. R. J. A Review of Block Polymer Surfactants. *J. Am. Oil Chem. Soc.* **1977**, *54*, 110–116.
- (2) Hamley, I. W. *Block Copolymers in Solution: Fundamentals and Applications*; Wiley & Sons, 2005.
- (3) Mali, K. S.; Dutt, G. B.; Mukherjee, T. Polyene Photoisomerization Rates: Are They Distinct in Aqueous Block Copolymer Micellar Solutions and Gels? *J. Chem. Phys.* **2006**, *124*, 054904–054910.
- (4) Dutt, G. B. How Critical Micelle Temperature Influences Rotational Diffusion of Hydrophobic Probes Solubilized in Aqueous Triblock Copolymer Solutions. *J. Phys. Chem. B* **2005**, *109*, 4923–4928.
- (5) Ghosh, S.; Adhikari, A.; Mandal, U.; Dey, S.; Bhattacharyya, K. Excitation Wavelength Dependence of Solvation Dynamics in a Gel. (PEO)₂₀-(PPO)₇₀-(PEO)₂₀ Triblock Copolymer. *J. Phys. Chem. C* **2007**, *111*, 8775–8780.
- (6) Wanka, G.; Hoffmann, H.; Ulbricht, W. Phase Diagrams and Aggregation Behavior of Poly(oxyethylene)-Poly(oxypropylene)-Poly(oxyethylene) Triblock Copolymers in Aqueous Solutions. *Macromolecules* **1994**, *27*, 4145–4159.
- (7) Alexandridis, P.; Holzwarth, J. F.; Hatton, T. A. Micellization of Poly(ethylene Oxide)-Poly(propylene Oxide)-Poly(ethylene Oxide) Triblock Copolymers in Aqueous Solutions: Thermodynamics of Copolymer Association. *Macromolecules* **1994**, *27*, 2414–2425.
- (8) Holmqvist, P.; Alexandridis, P.; Lindman, B. Modification of the Microstructure in Block Copolymer–Water–“Oil” Systems by Varying the Copolymer Composition and the “Oil” Type: Small-Angle X-Ray Scattering and Deuterium-NMR Investigation. *J. Phys. Chem. B* **1998**, *102*, 1149–1158.
- (9) Ghosh, S.; Mandal, U.; Adhikari, A.; Bhattacharyya, K. Study of Diffusion of Organic Dyes in a Triblock Copolymer Micelle and Gel by Fluorescence Correlation Spectroscopy. *Chem. - Asian J.* **2009**, *4*, 948–954.
- (10) Mali, K. S.; Dutt, G. B.; Mukherjee, T. Photoisomerization of a Carbocyanine Derivative in the Reverse Phases of a Block Copolymer: Evidence for the Existence of Water Droplets. *Langmuir* **2006**, *22*, 6837–6842.
- (11) Prabhhu, S. R.; Dutt, G. B. Solute Dynamics in Block-Copolymer Reverse Micelles: Do Water Content and Copolymer Concentration Alter the Microenvironment? *J. Chem. Phys.* **2014**, *140*, 234905–234912.
- (12) Zhao, C.; Winnik, M. A.; Riess, G.; Croucher, M. D. Fluorescence Probe Techniques Used To Study Micelle Formation in Water-Soluble Block Copolymers. *Langmuir* **1990**, *6*, 514–516.
- (13) Kundu, A.; Verma, P. K.; Ha, J.-H.; Cho, M. Studying Water Hydrogen-Bonding Network near the Lipid Multibilayer with Multiple IR Probes. *J. Phys. Chem. A* **2017**, *121*, 1435–1441.
- (14) van der Post, S. T.; Bakker, H. J. The Combined Effect of Cations and Anions on the Dynamics of Water. *Phys. Chem. Chem. Phys.* **2012**, *14*, 6280–6288.
- (15) Sagle, L. B.; Zhang, Y.; Litosh, V. A.; Chen, X.; Cho, Y.; Cremer, P. S. Investigating the Hydrogen-Bonding Model of Urea Denaturation. *J. Am. Chem. Soc.* **2009**, *131*, 9304–9310.
- (16) Sagle, L. B.; Cimatu, K.; Litosh, V. A.; Liu, Y.; Flores, S. C.; Chen, X.; Yu, B.; Cremer, P. S. Methyl Groups of Trimethylamine N-Oxide Orient Away from Hydrophobic Interfaces. *J. Am. Chem. Soc.* **2011**, *133*, 18707–18712.
- (17) Verma, P. K.; Lee, H.; Park, J. Y.; Lim, J. H.; Maj, M.; Choi, J. H.; Kwak, K. W.; Cho, M. Modulation of the Hydrogen Bonding Structure of Water by Renal Osmolytes. *J. Phys. Chem. Lett.* **2015**, *6*, 2773–2779.
- (18) Verma, P. K.; Kundu, A.; Ha, J.; Cho, M. Water Dynamics in Cytoplasm-Like Crowded Environment Correlates with the Conformational Transition of the Macromolecular Crowder. *J. Am. Chem. Soc.* **2016**, *138*, 16081–16088.
- (19) Moilanen, D. E.; Spry, D. B.; Fayer, M. D. Water Dynamics and Proton Transfer in Nafion Fuel Cell Membranes. *Langmuir* **2008**, *24*, 3690–3698.
- (20) Kundu, A.; Kwak, K.; Cho, M. Water Structure at the Lipid Multibilayer Surface: Anionic Versus Cationic Head Group Effects. *J. Phys. Chem. B* **2016**, *120*, S002–S007.
- (21) Kundu, A.; Blasiak, B.; Lim, J. H.; Kwak, K.; Cho, M. Water Hydrogen-Bonding Network Structure and Dynamics at Phospholipid Multibilayer Surface: Femtosecond Mid-IR Pump-Probe Spectroscopy. *J. Phys. Chem. Lett.* **2016**, *7*, 741–745.
- (22) Groot, C. C. M.; Velikov, K. P.; Bakker, H. J. Structure and Dynamics of Water Molecules Confined in Triglyceride Oils. *Phys. Chem. Chem. Phys.* **2016**, *18*, 29361–29368.
- (23) Fenn, E. E.; Moilanen, D. E.; Levinger, N. E.; Fayer, M. D. Water Dynamics and Interactions in Water-Polyether Binary Mixtures. *J. Am. Chem. Soc.* **2009**, *131*, 5530–5539.
- (24) Rezus, Y. L. A.; Bakker, H. J. Observation of Immobilized Water Molecules around Hydrophobic Groups. *Phys. Rev. Lett.* **2007**, *99*, 148301–148305.
- (25) Rezus, Y. L. A.; Bakker, H. J. Strong Slowing down of Water Reorientation in Mixtures of Water and Tetramethylurea. *J. Phys. Chem. A* **2008**, *112*, 2355–2361.

- (26) Piletic, I. R.; Tan, H. S.; Fayer, M. D. Dynamics of Nanoscopic Water: Vibrational Echo and Infrared Pump-Probe Studies of Reverse Micelles. *J. Phys. Chem. B* **2005**, *109*, 21273–21284.
- (27) Piletic, I. R.; Moilanen, D. E.; Spry, D. B.; Levinger, N. E.; Fayer, M. D. Testing the Core/shell Model of Nanoconfined Water in Reverse Micelles Using Linear and Nonlinear IR Spectroscopy. *J. Phys. Chem. A* **2006**, *110*, 4985–4999.
- (28) Bakulin, A. A.; Pshenichnikov, M. S. Reduced Coupling of Water Molecules near the Surface of Reverse Micelles. *Phys. Chem. Chem. Phys.* **2011**, *13*, 19355–19361.
- (29) Bakulin, A. A.; Cringus, D.; Pieniazek, P. A.; Skinner, J. L.; Jansen, T. L. C.; Pshenichnikov, M. S. Dynamics of Water Confined in Reversed Micelles: Multidimensional Vibrational Spectroscopy Study. *J. Phys. Chem. B* **2013**, *117*, 15545–15558.
- (30) Kumar, S. K. K.; Tamimi, A.; Fayer, M. D. Dynamics in the Interior of AOT Lamellae Investigated with Two-Dimensional Infrared Spectroscopy. *J. Am. Chem. Soc.* **2013**, *135*, 5118–5126.
- (31) Cringus, D.; Bakulin, A. A.; Lindner, J.; Vöhringer, P.; Pshenichnikov, M. S.; Wiersma, D. A. Ultrafast Energy Transfer in Water-AOT Reverse Micelles. *J. Phys. Chem. B* **2007**, *111*, 14193–14207.
- (32) Zhao, W.; Moilanen, D. E.; Fenn, E. E.; Fayer, M. D. Water at the Surfaces of Aligned Phospholipid Multibilayer Model Membranes Probed with Ultrafast Vibrational Spectroscopy. *J. Am. Chem. Soc.* **2008**, *130*, 13927–13937.
- (33) Kel, O.; Tamimi, A.; Thielges, M. C.; Fayer, M. D. Ultrafast Structural Dynamics inside Planar Phospholipid Multibilayer Model Cell Membranes Measured with 2D IR Spectroscopy. *J. Am. Chem. Soc.* **2013**, *135*, 11063–11074.
- (34) Moilanen, D. E.; Piletic, I. R.; Fayer, M. D. Tracking Water's Response to Structural Changes in Nafion Membranes. *J. Phys. Chem. A* **2006**, *110*, 9084–9088.
- (35) Kropman, M. F.; Bakker, H. J. Effect of Ions on the Vibrational Relaxation of Liquid Water. *J. Am. Chem. Soc.* **2004**, *126*, 9135–9141.
- (36) Fayer, M. D.; Moilanen, D. E.; Wong, D.; Rosenfeld, D. E.; Fenn, E. E.; Park, S. Water Dynamics in Salt Solutions Studied with Ultrafast Two-Dimensional Infrared (2D-IR) Vibrational Echo Spectroscopy. *Acc. Chem. Res.* **2009**, *42*, 1210–1219.
- (37) Choi, J. H.; Kim, H.; Kim, S.; Lim, S.; Chon, B.; Cho, M. Ion Aggregation in High Salt Solutions. III. Computational Vibrational Spectroscopy of HDO in Aqueous Salt Solutions. *J. Chem. Phys.* **2015**, *142*, 204102–204115.
- (38) Nicodemus, R. A.; Corcelli, S. A.; Skinner, J. L.; Tokmakoff, A. Collective Hydrogen Bond Reorganization in Water Studied with Temperature-Dependent Ultrafast Infrared Spectroscopy. *J. Phys. Chem. B* **2011**, *115*, 5604–5616.
- (39) Schmidt, J. R.; Corcelli, S. A.; Skinner, J. L. Pronounced Non-Condon Effects in the Ultrafast Infrared Spectroscopy of Water. *J. Chem. Phys.* **2005**, *123*, 044513–044526.
- (40) Jeon, J.; Lim, J. H.; Kim, S.; Kim, H.; Cho, M. Simultaneous Spectral and Temporal Analyses of Kinetic Energies in Non-equilibrium Systems: Theory and Application to Vibrational Relaxation of O-D Stretch Mode of HOD in Water. *J. Phys. Chem. A* **2015**, *119*, 5356–5367.
- (41) Oxtoby, D. W. Vibrational Relaxation in Liquids. *Annu. Rev. Phys. Chem.* **1981**, *32*, 77–101.
- (42) Rezus, Y. L. A.; Bakker, H. J. Orientational Dynamics of Isotopically Diluted H₂O and D₂O. *J. Chem. Phys.* **2006**, *125*, 144512–144521.
- (43) Kim, S.; Kim, H.; Choi, J. H.; Cho, M. Ion Aggregation in High Salt Solutions: Ion Network versus Ion Cluster. *J. Chem. Phys.* **2014**, *141*, 124510–124525.
- (44) Torii, H. Time-Domain Calculations of the Polarized Raman Spectra, the Transient Infrared Absorption Anisotropy, and the Extent of Delocalization of the OH Stretching Mode of Liquid Water. *J. Phys. Chem. A* **2006**, *110*, 9469–9477.
- (45) Kropman, M. F.; Nienhuys, H. K.; Woutersen, S.; Bakker, H. J. Vibrational Relaxation and Hydrogen-Bond Dynamics of HDO: H₂O. *J. Phys. Chem. A* **2001**, *105*, 4622–4626.
- (46) Smit, W. J.; Bakker, H. J. Anomalous Temperature Dependence of the Vibrational Lifetime of the OD Stretch Vibration in Ice and Liquid Water. *J. Chem. Phys.* **2013**, *139*, 204504–204510.
- (47) Fenn, E. E.; Wong, D. B.; Fayer, M. D. Water Dynamics at Neutral and Ionic Interfaces. *Proc. Natl. Acad. Sci. U. S. A.* **2009**, *106*, 15243–15248.
- (48) Moilanen, D. E.; Levinger, N. E.; Spry, D. B.; Fayer, M. D. Confinement or the Nature of the Interface? Dynamics of Nanoscopic Water. *J. Am. Chem. Soc.* **2007**, *129*, 14311–14318.
- (49) Laage, D.; Hynes, J. T. A Molecular Jump Mechanism of Water Reorientation. *Science* **2006**, *311*, 832–835.
- (50) Laage, D.; Hynes, J. T. Reorientational Dynamics of Water Molecules in Anionic Hydration Shells. *Proc. Natl. Acad. Sci. U. S. A.* **2007**, *104*, 11167–11172.
- (51) Packwood, D. M.; Han, P.; Hitosugi, T. Chemical and Entropic Control on the Molecular Self-Assembly Process. *Nat. Commun.* **2017**, *8*, 14463–14471.
- (52) Paci, E.; Karplus, M. Unfolding Proteins by External Forces and Temperature: The Importance of Topology and Energetics. *Proc. Natl. Acad. Sci. U. S. A.* **2000**, *97*, 6521–6526.
- (53) Georg, H.; Siebert, F. *Temperature Induced Protein Unfolding and Refolding Studied by Time-Resolved Infrared Spectroscopy*; Springer Netherlands: Dordrecht, 1997.
- (54) Hiemenz, P. C. *Principles of Colloid and Surface Chemistry*, 2nd ed.; Marcel Dekker: New York, 1986.